NASA Technical Memorandum

NASA TM- 103589

THE EFFECT OF INDUCED CHARGES ON LOW-ENERGY PARTICLE TRAJECTORIES NEAR CONDUCTING AND SEMICONDUCTING PLATES

By Victoria N. Coffey and Thomas E. Moore

Space Science Laboratory
Science and Engineering Directorate

May 1992

National Aeronautics and Space Administration

George C. Marshall Space Flight Center

TABLE OF CONTENTS

LIST OF ILLUSTRATIONS

TECHNICAL MEMORANDUM

THE EFFECT OF INDUCED CHARGES ON LOW-ENERGY PARTICLE TRAJECTORIES NEAR CONDUCTING AND SEMICONDUCTING SURFACES

I. INTRODUCTION

With the attention toward increasingly lower energy (<50 eV) ion behavior in the magnetosphere,[1] there is a greater emphasis placed on the focusing properties of space plasma instruments designed to measure the flux of very low-energy ions. This need comes simultaneously as instrumentation development permits better resolution and with the capability to control spacecraft charging and differential charging. [2] Often in these instruments, the particle energies are selected electrostatically and their arrival angle, if determined, can be selected either electrostatically [3] or by collimation. [4] Using these techniques to measure low-energy particles, conditions arise that may cause particle trajectories to vary from their ideal path in the instrument. For example, the analysis of low-energy ions with retarding potential grids is often seriously affected by space charge and stray electric and magnetic fields. [5]

The process that will be focused on in this paper is the effect of induced charges on low-energy particles as they travel near conducting and semiconducting surfaces. In particular, the question to be answered is the effect of the induced charge on these particles as they pass through grounded channels that are similar in dimension to those that may be designed in space plasma instruments. The Thermal Ion Dynamics Experiment (TIDE) on the future Global Geoscience (GGS) mission is designed to have an array of beryllium copper channels to serve as angle collimators for incident particles, each channel having a height of 1.27 mm, length of 25.4 mm, and thus a length to width ratio of 20. Another example occurs in a design by Stenzel in which he replaces the first grid of a retarding potential analyzer with a grounded microchannel plate (MCP) resulting in a vary narrow angular response. The MCP is a honeycomb-like structure of hollow glass channels that are treated in such a way as to render the channel walls semiconducting with a resistivity ranging from 10^{10} to 10^{15} Ω cm. Typically these glass channels have internal diameters ranging from 0.01 to 0.1 mm and length to diameter ratios ranging from 40 to 100.

To answer the question posed above, a computer model was developed to inject singly charged particles into channels of both grounded, conducting plates, and semiconducting plates. The induced charge on the particles was then found by using the method of images. The dielectric constant for the semiconducting plates was $\varepsilon = 8.3$, the same constant for the Corning 8161 glass used in MCP plates provided by Galileo. [6] To study the effect of the induced charges various geometric parameters were varied: the parallel plates, ranged in length from 0.1 mm to 50 mm, the aspect ratio, defined here as the plate length to the separation of the plates, ranged from 1 to 100, and the distance of the simulated detector from the end of the plates varied.

In the following, the design of the computer simulation will first be discussed, examples of particle trajectories with and without the force of induced charges will be shown, and results will be given on the effected channel geometric factor.

II. PROCEDURE

It is well known that for a point charge between parallel, grounded plates you can find the induced charge on the plates by the method of images. Although the problem can be solved by a wide variety of methods, [7-13] the method of images was chosen which is straightforward and can lead to an absolute and uniformly convergent series when treated carefully.

The parallel planes were chosen to be at the locations of $y = d/2$ and $y = -d/2$ and the charge was placed at an arbitrary distance, y, from the center of the channel (see Appendix A). To force the potential of the plane at $y = d/2$ to zero we place an image charge opposite in sign and symmetric to the plane, etc. Now to force the potential to zero on the plane at $y = -d/2$ we have to introduce two corresponding charges of opposite sign at the points symmetric to this plane, etc. An infinite series results and the series converges because each successive image decreases in magnitude. The resulting force on the charge q for conductive plates is

$$|F| = \frac{2hq^2}{\pi\varepsilon_o d^2} \sum_{j=1,3,5\ldots}^{\infty} \frac{j}{(j^2 - 4h^2)^2}$$

where j is the image pair index, d is the distance between the plates, and $h = y/d$. The force on the charge q using semiconductive plates with a dielectric constant of 8.3 is

$$|F| = \frac{1.57hq^2}{\pi\varepsilon_o d^2} \sum_{j=1,3,5\ldots}^{\infty} \frac{j}{(j^2 - 4h^2)^2}$$

(see Appendix A for the derivations). From these equations it can be seen that as j increases, the terms in the series decrease for a constant position of the particle. Also as seen from Appendix A, the even image pairs cancel so the sum is carried out over the odd values of j. For this study j was summed to 7 for the sake of computer efficiency. This introduced a percent error of less than 0.4 using an h of 0.01. Figure 1 shows a log-linear plot of the force as a function of h, showing the force on the particle is zero at the center of the channel, $h = 0$, and reaches infinity when the particle is near the plate at $h = 0.5$. This curve was derived using the force obtained from conductive plates.

The computer model was constructed so that particles were injected between simulated parallel plates at incremental position and angle steps so as to illuminate the channel with all possible trajectories (see Figure 2). Transmission was then determined for the initial conditions. The angles were limited to the range that allowed trajectories with the greatest angle of incidence, this maximum angle defined by $\alpha = tan^{-1}\, d/L$, where L is the length of the channel.

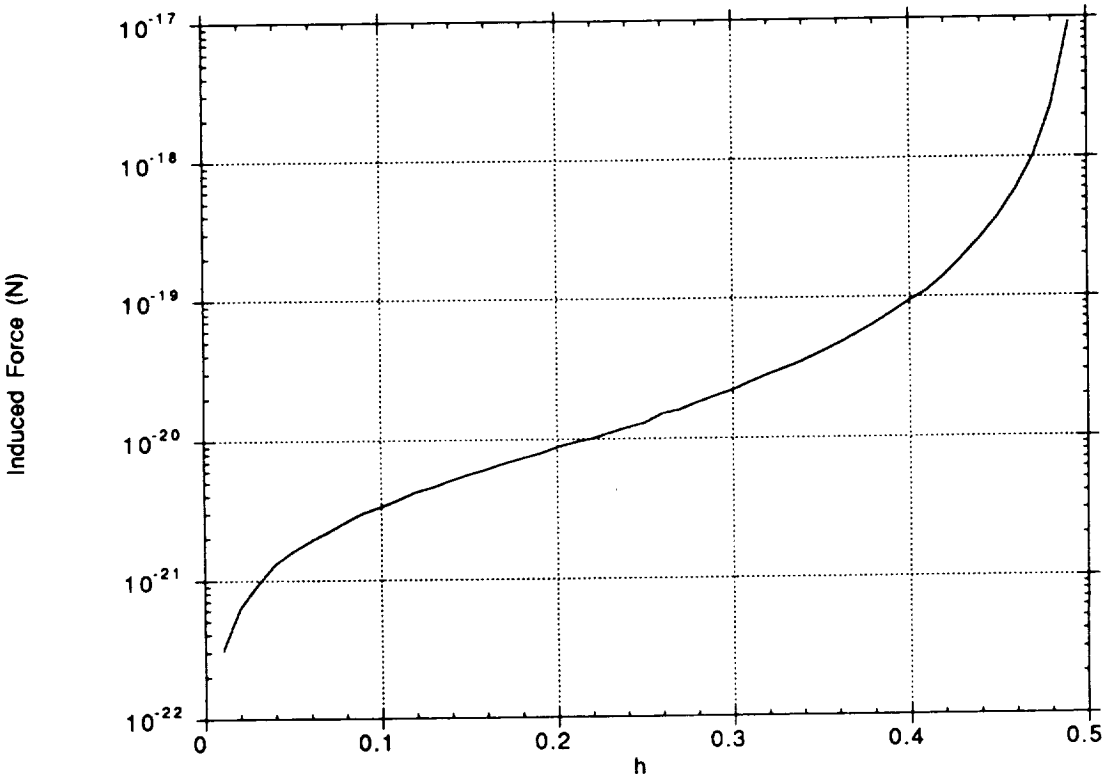

Fig.1. The induced force on a particle as a function of position in the channel.

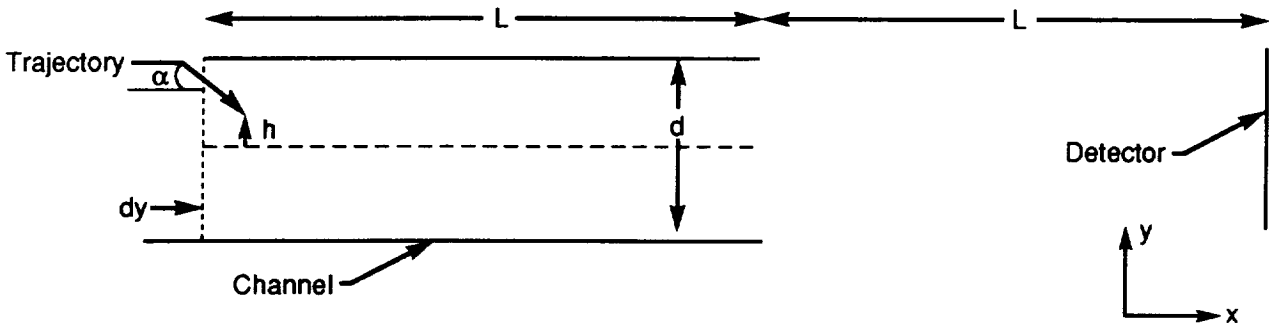

Fig. 2. Geometric construction of the simulation.

The positions of entry, *dy*, were held between 0 and *d*/2 due to the symmetry of the problem. The maximum for both angles and positions was divided into steps of 24 creating a 24 x 24 *dy*-α transmission matrix. To illustrate, beginning at the first entry position at the center of the channel, a particle was injected at each of the $\pm$12 angles, etc. The 25th particle then entered at the next entry position at the first angle, etc. The particles moved according to the equation of motion using the "leap frog" method in time steps resolved to 0.001 of their time to cross the channel. This resolution was a trade-off between accuracy of the trajectory and computer time. A simulated detector, the same width of the plate separation, was placed at the end of the channel. The distance of this detector from the end of the channel, or the force free region, was modeled in three different positions: flush to the channel or a distance of 1L or 2L from the end of the channel. Now with this simulation as just described, the parameters studied were the particle energy, the channel length, the aspect ratio, and the detector distance.

III. RESULTS

Figures 3 and 4 illustrate the effect of induced charges on representative low-energy particles as they pass through grounded, conducting channels. In these figures, the vertical axis shows the width of the channel and the detector, and the horizontal axis shows the center of the channel and extends to the detector. The channels in these two figures have a width of 0.25 mm, a length of 2.5 mm, and the detector is placed one length of the channel away at 5 mm. Both panels of Figure 3 show the same five particles of 10^{-3} eV entering at the same positions near the plate and having the same incident angles of -5° to 6°. Panel a displays the trajectories with no induced force and panel b displays these trajectories with the induced force. Note that with the induced force, four out of the five particles are counted by the detector, whereas the particles with no force are not transmitted to the detector. Panels a and b of Figure 4 illustrate the induced force on particles of different energies. Again both panels show particles of the same entry positions, this time near the center of the channel, with the arrival angles -1° to 2.5°, but the particles in panel a are 1 eV and those of panel b are 10^{-3} eV. As these particles pass through the channel you can see again, as in Figure 3, the stronger induced force as the particles near the plates.

The nature of the trajectories, as affected by the induced charges, is more evident in Figures 5 and 6. Figure 5 shows *dy*-α transmission matrices whose elements are entry position and angle differentials with an * in the element marking the transmission of particles with corresponding conditions. The columns are labeled by entry element, *dy*, and the rows by angle element, α. These matrices were developed using once again a channel length of 2.5 mm, a channel aspect ratio of 10, and with the detector one length of the channel away at 5.0 mm. Panel a shows the transmission of 10^{-2} eV particles with no induced force showing the characteristic window and panel b shows the transmission of 10^{-2} eV particles with the induced force. Panel b illustrates that particles that entered near the plate had to enter at a more negative angle (away from the plate) to be transmitted.

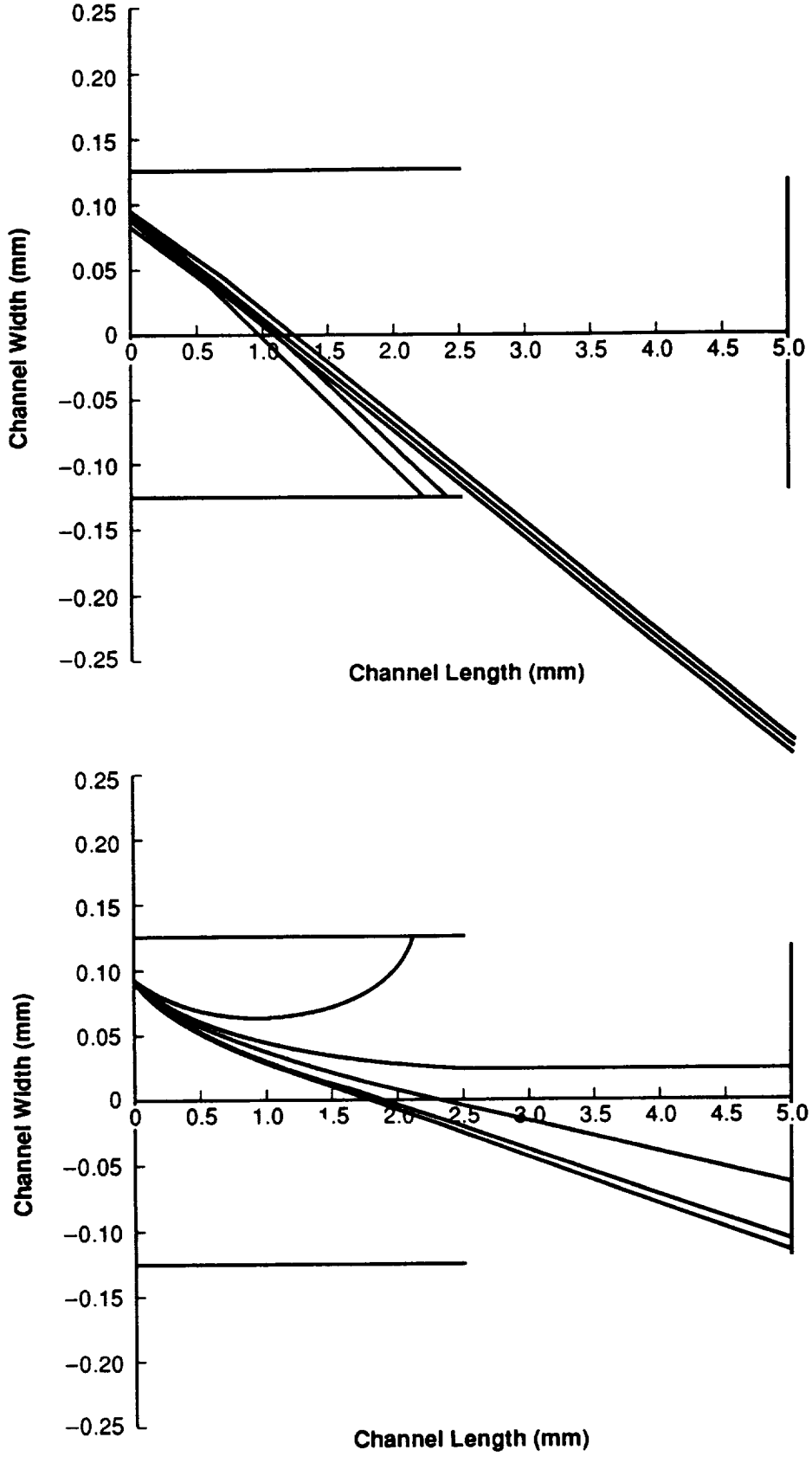

Fig. 3. Examples of the effect of the induced force on low-energy particle trajectories within a channel.

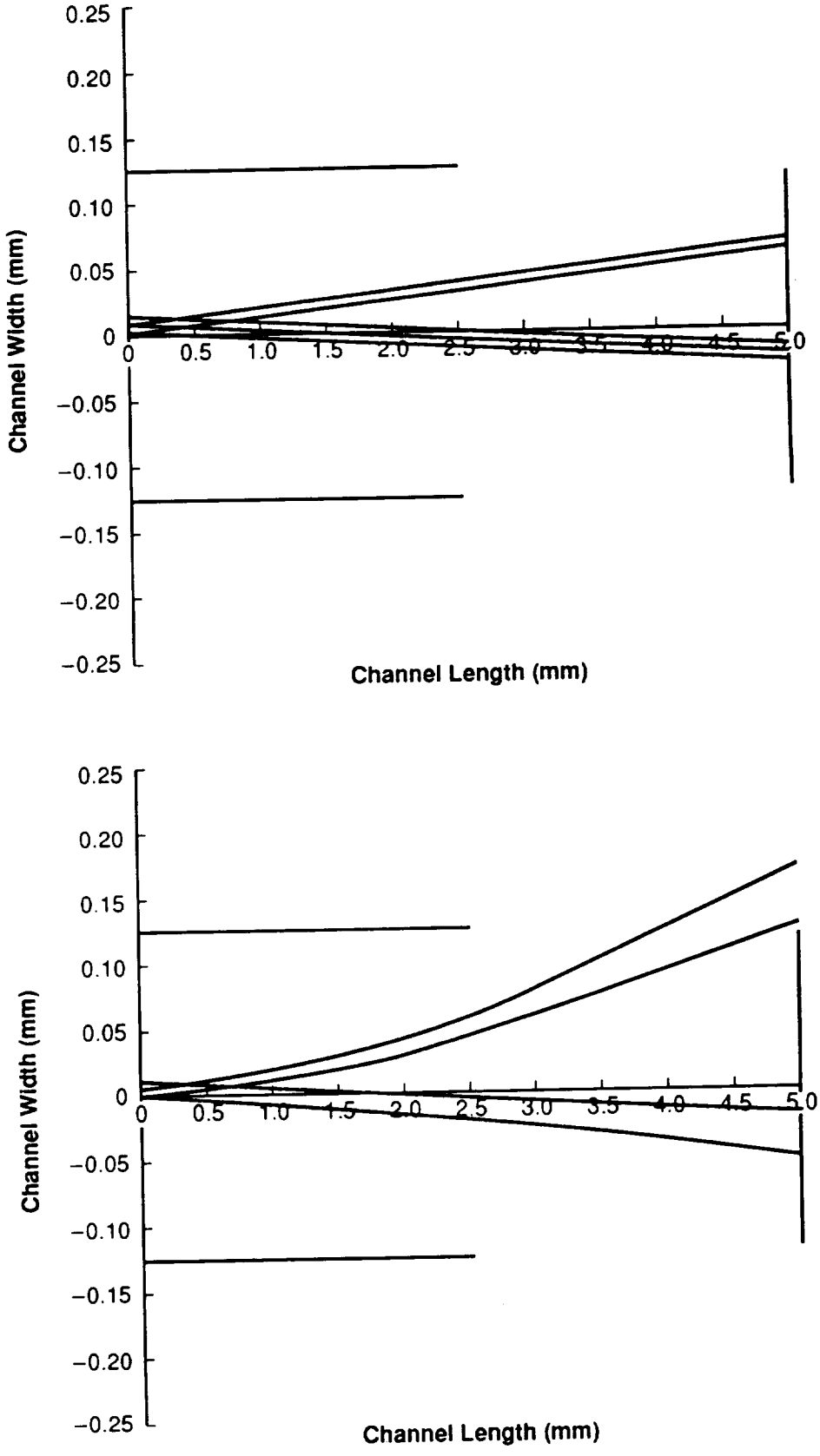

Fig. 4. Examples of the effect of the induced force with varying particle energies.

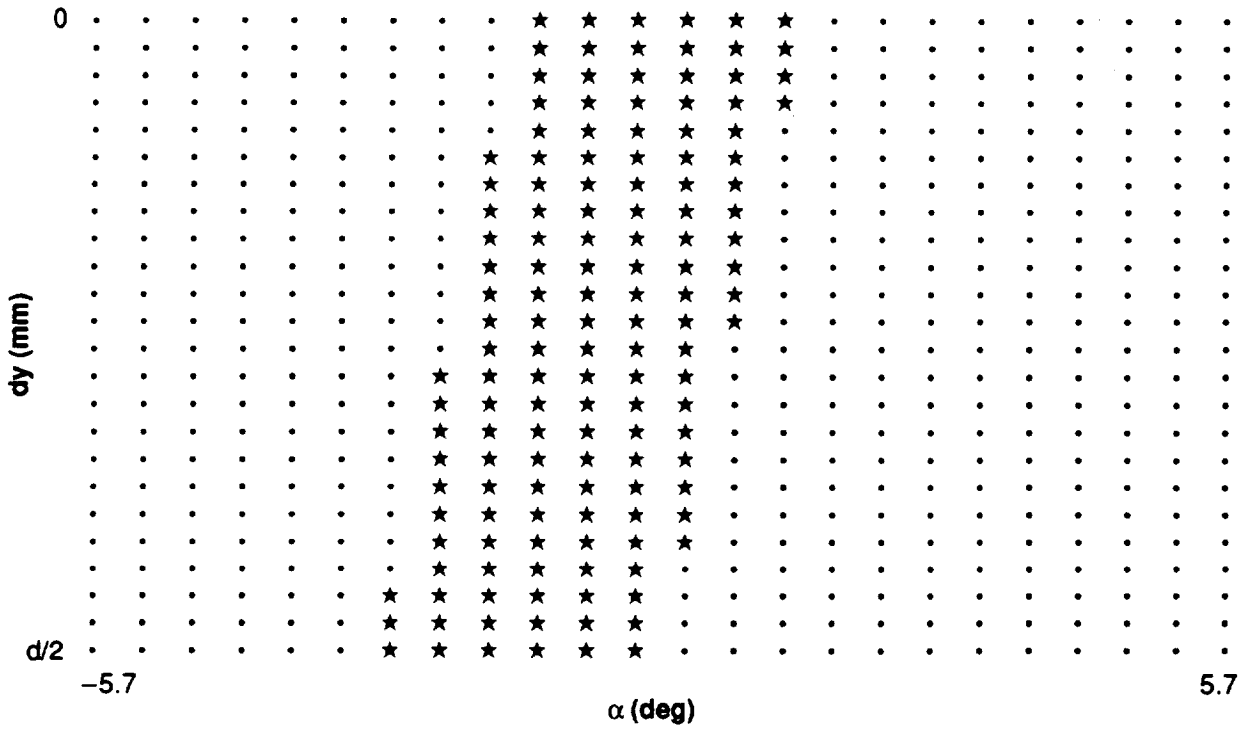

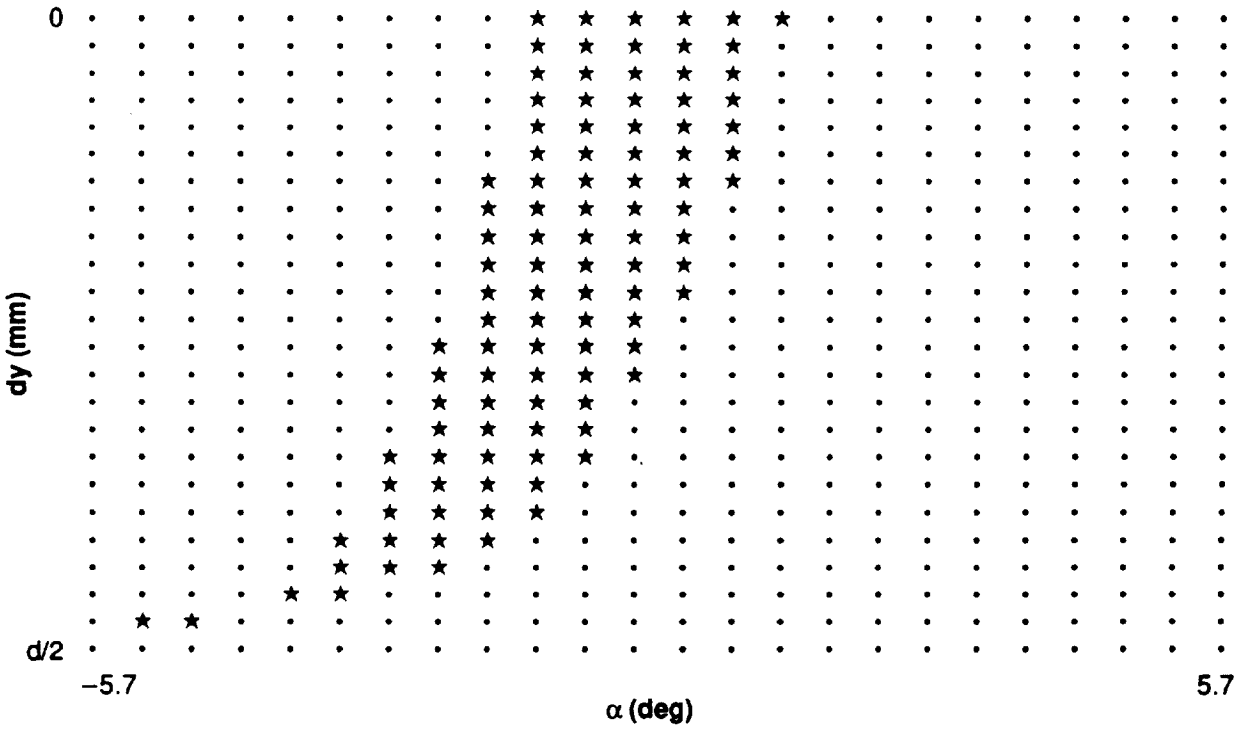

Fig. 5. Transmission matrices.

Figure 6 shows phase plots developed from the transmission matrices similar to Figure 5. The outside dotted region shows the area created by the 24 x 24 position and angle elements. The single striped region is the area created by passing the particles through the channel with no induced force as seen in Figure 5a, and the region overlayed, shown with cross-hatches, is created by passing the same particles through the channel with the induced force as in Figure 5b. Both panels of Figure 6 were obtained with the same channel geometry as in Figure 5 but panel a has particle energies of 10^{-2} eV while panel b has particle energies of 10^{-4} eV. Panel a shows a 27% reduction in transmission while panel b shows a 95% reduction.

To find the channel geometric factor as effected by the induced charge, we must know the relation of the number of particles CR (particles/accumulation) transmitted by the channel to the directional intensity, $I(y,\alpha,E)$, usually expressed in (particles/cm^2 sr eV accumulation). This relation is defined by

$$CR = \int I\, g(y,\alpha,E)\, dA\, d\Omega\, dE$$

where y is the position vector, α is the angle of incidence, and E is the particle energy. $g(y,\alpha,E)$ is a function in the energy-dependent geometric factor which will be defined for one dimension as

$$GF\,(E) = \int g(y,\alpha,E)\, dy\, d\alpha.$$

This quantity is a function of the efficiency and geometry of the analyzer/detector and is expressed in units of cm^2 sr. For the study, the function, g, has the value of 1 for values of y and α corresponding to trajectories which strike the detector and zero otherwise.

The 3D channel geometric factor can be obtained by resolving the particle motion due to the induced force into two perpendicular surfaces. Each calculation has the dimensions of length times angle, and then the total geometric factor is approximately the product of the two partial factors. This approximation is good for the small solid angles normally found in electrostatic analyzers. [14]

Figure 7 shows the effect of the induced charges on the energy-dependent geometric factor. This geometry factor is normalized by the geometric factor obtained using no induced force. These values were calculated using conductive plates. The dimensions of the channels used in both 7a and 7b have an aspect ratio of 10 but differ in that panel a has a channel length of 2.5 mm, while panel b has a channel length of 0.25 mm. The three curves from right to left mark the distance of the detector from the channel aperture; flush, 1L, and 2L, respectively. It can be seen by comparing both panels a and b that as the channel length decreases by a factor of 10 the particle energy has to increase by a factor of 10 to have the same geometric factor. Also note that at 1 eV the geometric factor is already reduced by 10%.

As a measure of the perceptibility of the induced charge effect, the value of the particle energy where the geometric factor fell by 50% was then plotted versus channel length ranging

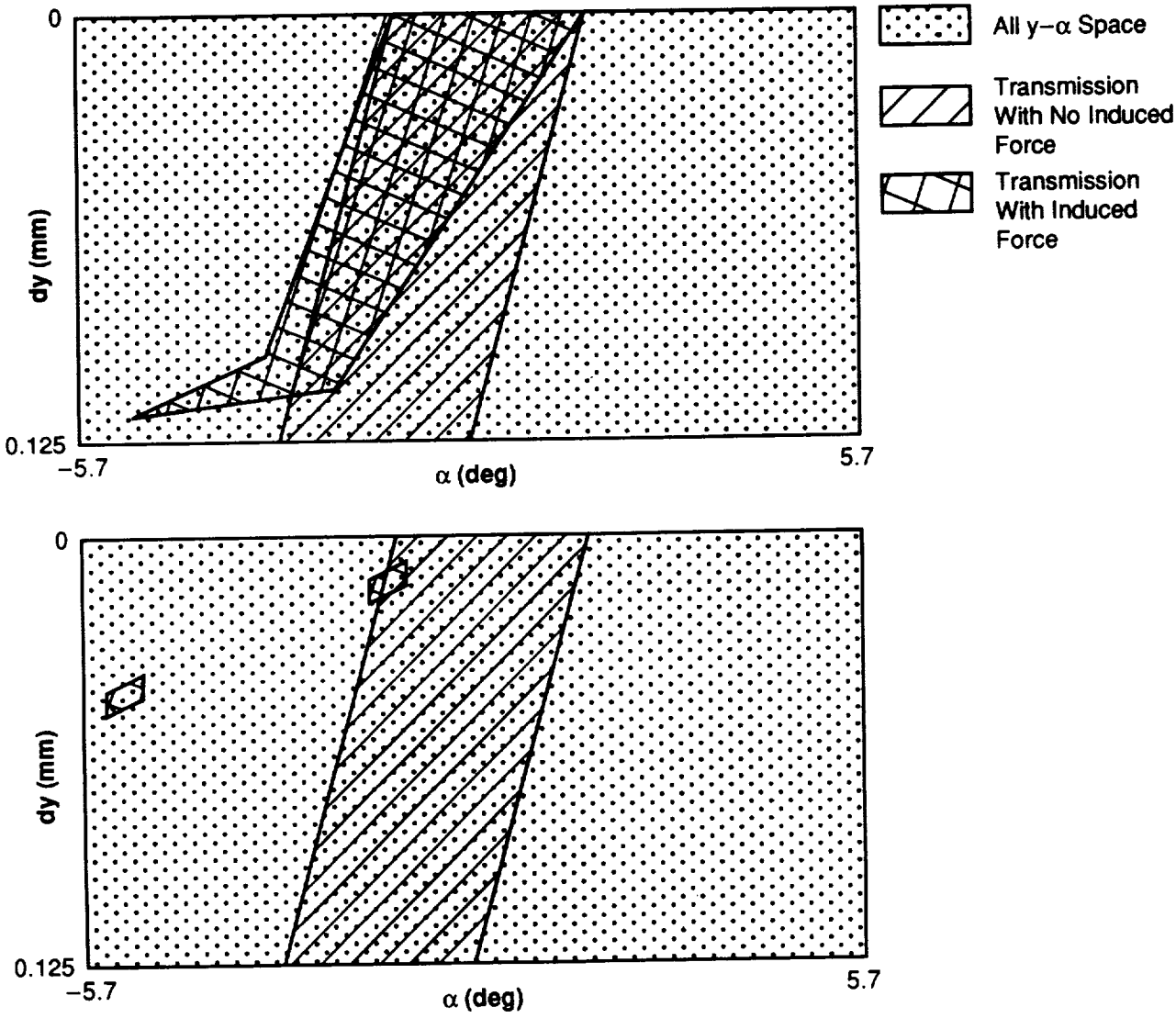

Fig. 6. Phase plots displaying the reduced area as a result of the induced force.

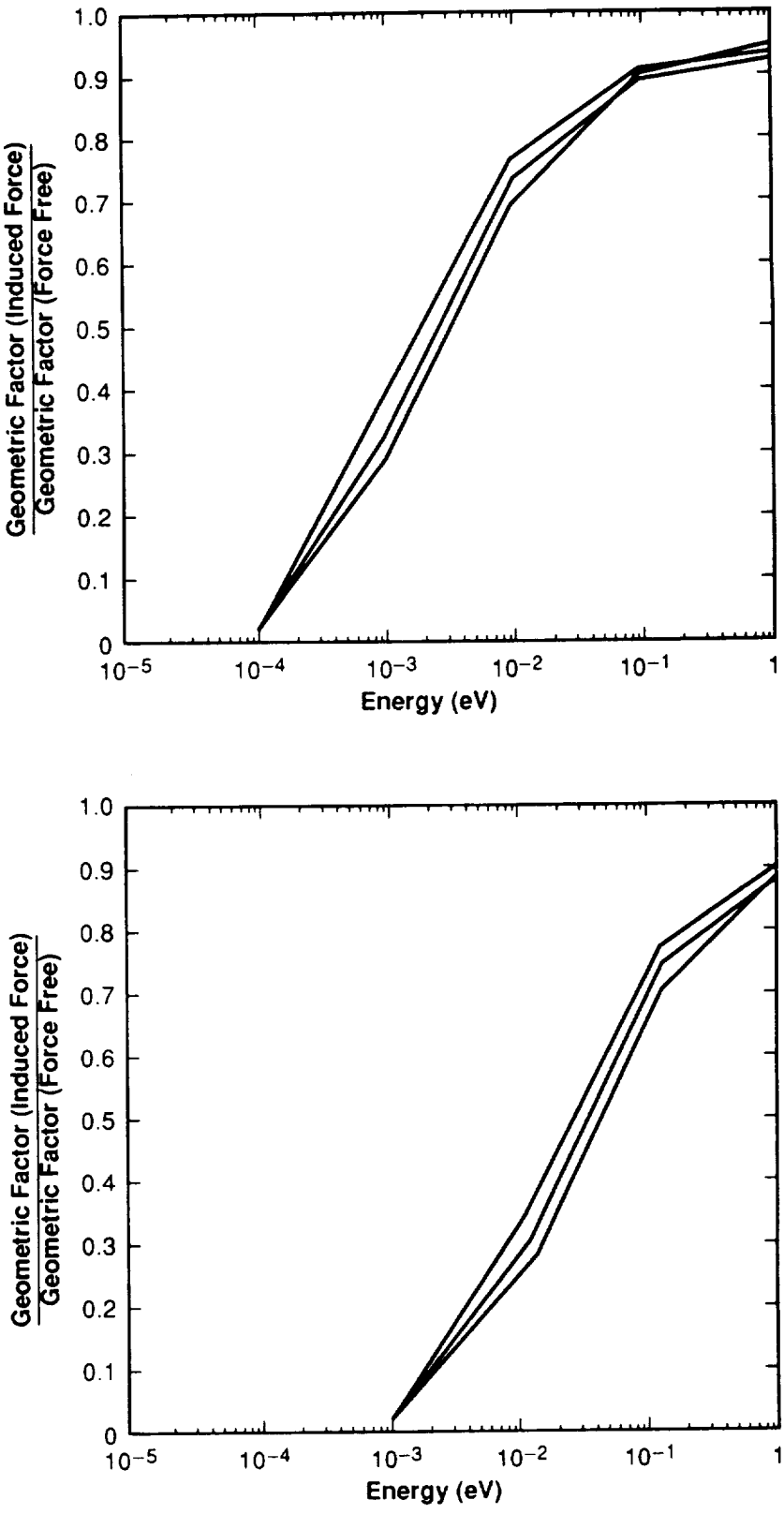

Fig. 7. Normalized geometric factor as a function of particle energy.

from 0.1 to 50 mm in Figure 8. This was done for both conducting and semiconducting channels with aspect ratios of 10. The energy value, denoted by $E_{0.5}$, is proportional to the length of the channel, L, by a constant and is defined as:

$$E_{0.5} = \frac{C}{L}$$

where C = 0.006 eV mm for conductors and

$$E_{0.5} = \frac{C_D}{L}$$

where C_D = 0.0046 eV mm for a semiconductor with a dielectric constant of 8.3. The detector is placed at $1L$ for each channel length where L is in mm.

Figure 9 shows the energy values plotted as a function of aspect ratio for both conductors and semiconductors. A relation between $E_{0.5}$ and channel dimension was found and can be used for any arbitrary channel. This relation is defined as

$$E_{0.5} = \frac{C}{L}\left(\frac{aspect\ ratio}{10}\right)^3$$

where C = 0.006 eV mm for conductors and

$$E_{0.5} = \frac{C_D}{L}\left(\frac{aspect\ ratio}{10}\right)^3$$

where C_D = 0.0046 eV mm for semiconductors.

IV. CONCLUSIONS

The induced force was found on particles as they passed through grounded, parallel plates which served as channels ranging in length from 0.1 to 50 mm and in aspect ratio from 1 to 100. This force was calculated for both conducting and semiconducting plates. The reduced geometric factor was found as a function of particle energy as the channel length, aspect ratio, and distance of the detector from the end of the channel was varied. Relations were obtained between the channel dimensions and the energy value where the geometry factor fell by 50%. For comparison, the angle collimators for TIDE have lengths of 25.4 mm and aspect ratios of 20. From the equations above we know that for conducting channels that $E_{0.5}$ will be 0.004 eV. For a grounded MCP with channel diameters of 50 μm and a length to diameter ratio of 60, $E_{0.5}$ is 0.3 eV. The results from this study show a need to consider the effect of induced charges on low-energy particles less than 1 eV as they near conducting or semiconducting surfaces for the channel dimensions cited. Although the channels of MCPs are weakly conducting, for these low energies and their small channel dimensions the induced force on the particle does need attention.

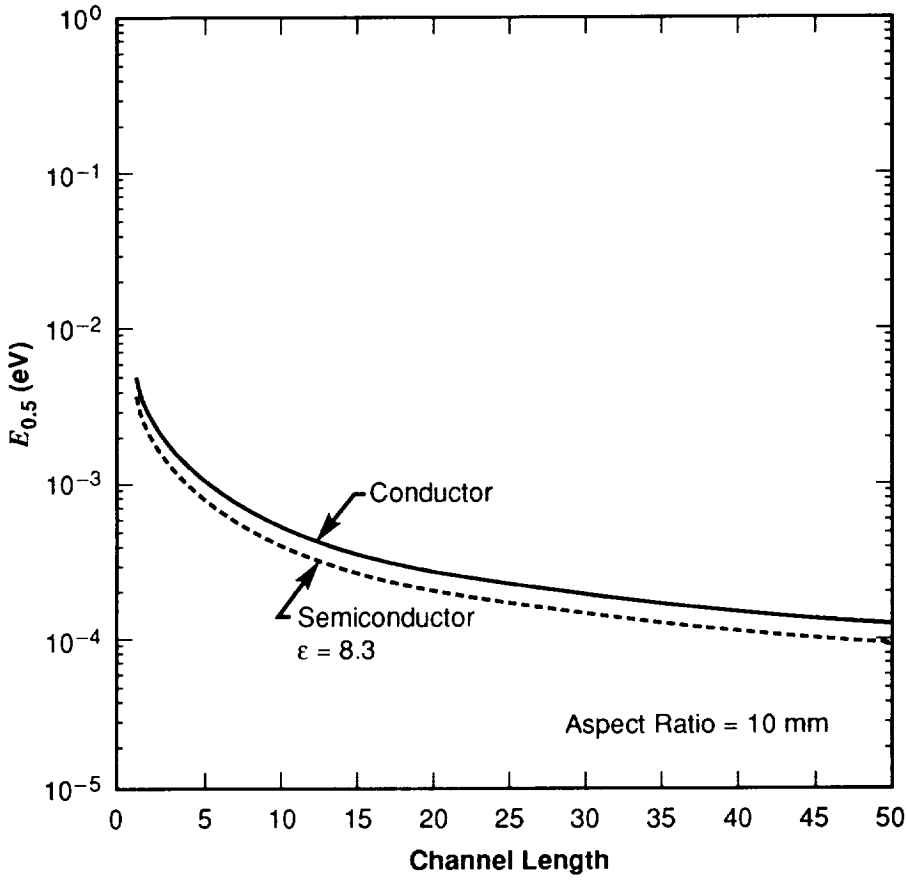

Figure 8. $E_{0.5}$ as a function of channel length.

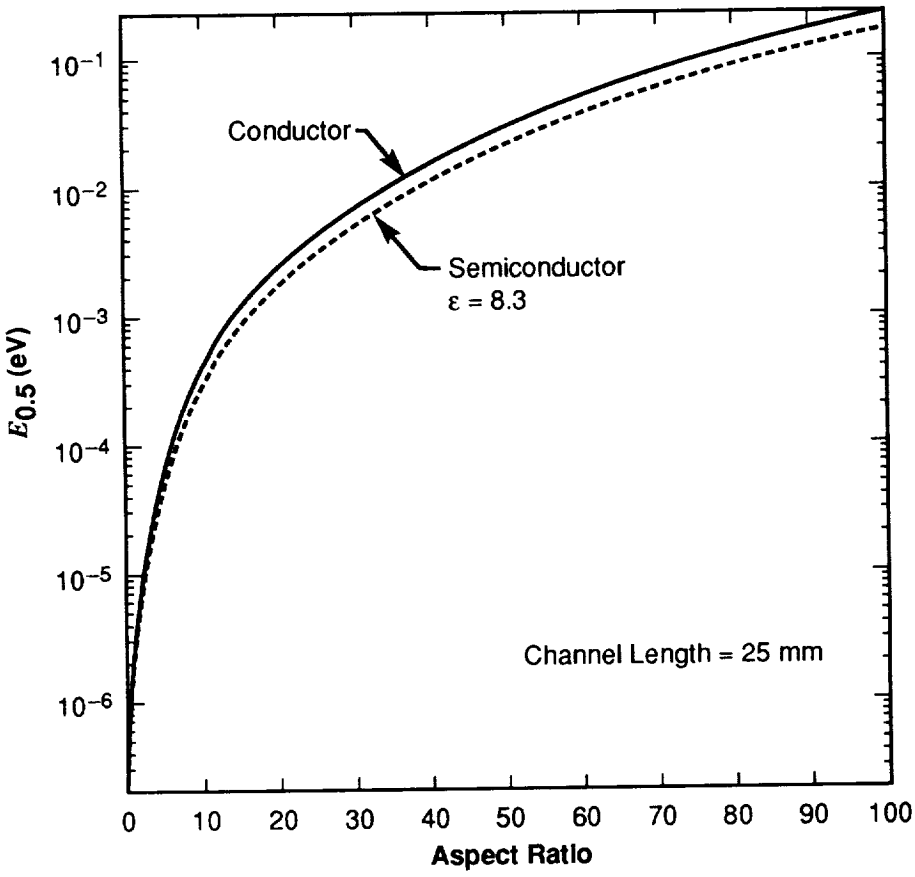

Figure 9. $E_{0.5}$ as a function of aspect ratio.

As a rule of thumb, the effect is appreciable at the 0.1 eV level for aspect ratios larger than 25 and lengths shorter than 1 mm.

REFERENCES

1. Horwitz, J.L: Core Plasma in the Magnetosphere, Geophys. Res. Lett. **25**, 579 (1987).

2. Whipple, E. C., Jr., The Problem of Low-Energy Particle Measurements, University of California, San Diego, Calif., 1978.

3. Stone, N. H.: Technique for Measuring the Differential Ion Flux Vector, Rev. Sci. Instrum. **48**, 1458 (1977).

4. Stenzel, R.L., Williams, R., Aguero, R., Kitazaki, K., Ling, A., McDonald, T., and Spitzer, J.: A Novel Directional Ion Energy Analyzer, Rev. Sci. Instrum. **53**, 1027 (1982).

5. Moore, J. H., Davis, C. C., and Coplan, M. A.: Building Scientific Apparatus, Addison-Wesley Publishing Company, 1983.

6. Wiza, J. L.: Microchannel Plate Dectectors, Nuclear Instruments & Methods **162**, 587-601 (1979).

7. Barrera, R. G., Guzman, O., and Balaguer B.: Point Charge in a Three-Dieletric Medium with Planar Interfaces, Am. J. Phys. **46**, 1172 (1978).

8. Dick, B. G.: Images and the Point Charge-Capacitor Problem, Am. J. Phys. **41**, 1289 (1973).

9. Fong C., and Kittel, C.: Induced Charge on Capacitor Plates, Am. J. Phys. **35**, 1091 (1967).

10. Kellogg, O. D.: Foundations of Potential Theory (Dover, New York, 1953), p. 230.

11. Pumplin, J.: Application of Sommerfeld-Watson Transformation to an Electrostatics Problem, Am. J. Phys. **37**, 737 (1969).

12. Scanio, J. J. G.: Green's Function and Images in an Electrostatics Problem, Am. J. Phys. **41**, 415 (1973).

13. Shockley, W.: Currents to Conductors Induced by a Moving Point Charge, J. Appl. Phys. **9**, 635 (1938).

14. Johnstone, A. D.: The Geometric Factor of a Cylindrical Plate Electrostatic Analyzer, Rev. Sci. Instrum. **43**, 1030 (1972).

15. Torre, E. D., and Longo, C. V.: The Electromagnetic Field (Allyn and Bacon, Inc., 1969).

Appendix A. Derivation of the Induced Force on a Charge Between Two Plates

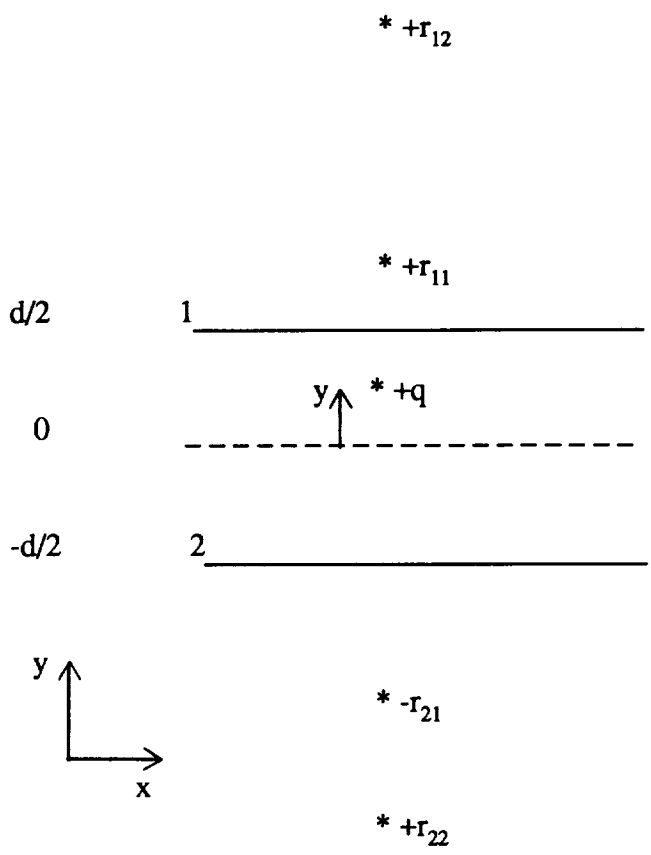

The plates coincide with the xz plane a distance d apart, and the point charge is at an arbitrary distance y above the center axis. The distance between the point charge and each image charge is r_{ij} where i is the number shown on the plates and j is the image pair index. The distance from the point charge of the first few images and their polarities are given below:

$r_{11} = d\text{-}2y$	attractive
$r_{21} = d\text{+}2y$	attractive
$r_{12} = 2d$	repulsive
$r_{22} = 2d$	repulsive
$r_{13} = 3d\text{-}2y$	attractive
$r_{23} = 3d\text{+}2y$	attractive
$r_{14} = 4d$	repulsive
$r_{24} = 4d$	repulsive

and so on...

Note that every even image pair cancels.

Using the equation

$$F = \frac{-q^2}{4\pi\varepsilon_o} \sum_{j=1}^{\infty} \left[\frac{1}{r_{1j^2}} - \frac{1}{r_{2j^2}} \right]$$

the resulting force on the charge, q, using conductive plates is

$$F = \frac{+q^2}{4\pi\varepsilon_o} \sum_{j=1,3,5...}^{\infty} \left[\left(\frac{1}{(jd-4y)^2} \right) - \left(\frac{1}{(jd+4y)^2} \right) \right]$$

where j is the image pair index. Simplifying, this equation becomes

$$F = \frac{+q^2}{4\pi\varepsilon_o} \sum_{j=1,3,5...}^{\infty} \frac{8jdy}{(j^2 d^2 - 4y^2)^2}$$

$$F = \frac{+2q^2 h}{\pi\varepsilon_o d^2} \sum_{j=1,3,5...}^{\infty} \frac{j}{(j^2 - 4h^2)^2}$$

where $h = \frac{y}{d}$.

To calculate the force on the charge, q, using dielectric boundaries, the image charges are replaced by $q\,(\varepsilon_1-\varepsilon_2/\varepsilon_1 + \varepsilon_2)$[15] where ε_1 is the permittivity within the channel and ε_2 is the permittivity of the dielectric boundary. The resulting force is

$$F = \frac{q^2}{4\pi\varepsilon_1} \left(\frac{\varepsilon_1 - \varepsilon_2}{\varepsilon_1 + \varepsilon_2} \right) \sum_{j=1,3,5...}^{\infty} \frac{8jdy}{(j^2 d^2 - 4y^2)^2}$$

$$F = \frac{0.785(2)q^2 h}{\pi\varepsilon_1 d^2} \sum_{j=1,3,5...}^{\infty} \frac{j}{(j^2 - 4h^2)^2}$$

$$F = \frac{1.57q^2 h}{\pi\varepsilon_1 d^2} \sum_{j=1,3,5...}^{\infty} \frac{j}{(j^2 - 4h^2)^2}$$

REPORT DOCUMENTATION PAGE

Form Approved
OMB No. 0704-0188

1. AGENCY USE ONLY (Leave blank)	2. REPORT DATE	3. REPORT TYPE AND DATES COVERED
	May 1992	Technical Memorandum

4. TITLE AND SUBTITLE

The Effect of Induced Charges on Low-Energy Particle Trajectories Near Conducting and Semiconducting Plates

5. FUNDING NUMBERS

6. AUTHOR(S)

Victoria N. Coffey and Thomas E. Moore

7. PERFORMING ORGANIZATION NAME(S) AND ADDRESS(ES)

George C. Marshall Space Flight Center
Marshall Space Flight Center, AL 35812

8. PERFORMING ORGANIZATION REPORT NUMBER

9. SPONSORING / MONITORING AGENCY NAME(S) AND ADDRESS(ES)

National Aeronautics and Space Administration
Washington, D.C. 20546

10. SPONSORING / MONITORING AGENCY REPORT NUMBER

NASA TM- 103589

11. SUPPLEMENTARY NOTES

Prepared by Space Science Laboratory, Science and Engineering Directorate.

12a. DISTRIBUTION / AVAILABILITY STATEMENT

Unclassified--Unlimited

12b. DISTRIBUTION CODE

13. ABSTRACT *(Maximum 200 words)*

The effect of the induced charge was found on particles less than 1 eV as they passed through simulated parallel, grounded channels that are comparable in dimension to those that are presently in space plasma instruments which measure the flux of low-energy ions. Applications were made to both conducting and semiconducting channels that ranged in length from 0.1 to 50 mm and in aspect ratio from 1 to 100. The effect of the induced charge on particle trajectories is illustrated and results are given for the reduction of the channel geometric factor as a function of particle energy due to the deviation of trajectories from simple straight lines. Several configurations of channel aspect ratio and detector locations are considered. The effect is important only at very low energies with small dimensions.

14. SUBJECT TERMS

Induced charge, geometric factor, low-energy particles, method of images

15. NUMBER OF PAGES

23

16. PRICE CODE

NTIS

17. SECURITY CLASSIFICATION OF REPORT	18. SECURITY CLASSIFICATION OF THIS PAGE	19. SECURITY CLASSIFICATION OF ABSTRACT	20. LIMITATION OF ABSTRACT
Unclassified	Unclassified	Unclassified	Unlimited